CHAPTER FIFTY FOUR

# SHOALING PROPERTIES OF BOUNDED LONG WAVES

E.P.D. Mansard* and V. Barthel*

ABSTRACT

Group bounded long waves which appear as a set-down under a group of high waves and a set-up in between groups are well described for constant water depth. However, their propagation into shallow water and their interaction with the constituent wave groups are not well understood and theoretically described yet. Therefore, model investigations were carried out to study shoaling properties of these second order waves in terms of amplitudes and phases. The tests give a good insight into the phenomenon and suggest distinct shoaling properties. Moreover, experimental results provide a valuable basis for future theoretical considerations.

## 1.0 INTRODUCTION

Recent investigations have shown that model tests of harbour basins and moored ships are highly dependent on the correct reproduction of grouped sea states. Using the concept of radiation stress, Longuet-Higgins and Stewart (4) have established that a set-down of the mean water level occurs under wave groups with a corresponding set-up in between the groups. This results in a variation of the mean water level known as a Bounded Long Wave (BLW) with its period equal to that of the wave groups. The Bounded Long Wave, which travels with the group velocity, is of second order and therefore cannot be reproduced in a model just by application of the first order classical wave generation, since the boundary conditions required at the paddle are not being satisfied. As a consequence the following spurious long wave components are generated in a model in addition to the inevitably produced Bounded Long Wave:

- a free parasitic long wave which is opposite in phase to the bounded long wave,
- a free displacement wave generated due to the moving boundary of the paddle, and
- a free long wave generated by the first order local disturbances (negligible amplitude with respect to the above two).

These spurious long waves, which propagate at free wave celerities, can travel back and forth along the flume since they are almost fully reflected even from beaches with mild slopes. The resulting standing wave system could therefore lead to incorrect and unrealistic responses of test structures depending on their location. However, these free long waves can be reduced by including correct suppression terms in the

*Hydraulics Laboratory, National Research Council, Ottawa, Ont. K1A 0R6 Canada

wave generation. This is basically achieved by generating, along with first order waves, long wave components which are equal in amplitude but opposite in phase to those spurious contributions. The theoretical expressions of these contributions are given by Ottensen-Hansen et al. (6) and their successful suppression in a physical model is demonstrated by Barthel et al. (1). These suppression techniques used in model investigations of moored ship response (Mansard and Pratte) (5) and wave run-up on beaches (Barthel et al.) (2) have clearly established their importance in obtaining a realistic response of the structure in the model.

## 2.0 OBJECTIVES

This paper describes the continuation of the research program and deals with the shoaling properties of the group-bound long waves. Although these waves are small in amplitude, their shoaling effects can significantly influence the model response. Harbour oscillations are one of the examples where these effects can be greatly felt: the long waves penetrating the harbour can induce long period seiches or resonance causing thereby enhanced slow drift motions of moored vessels or other floating structures.

At present there is no description (either theoretical or experimental) of the shoaling properties of these waves. Model investigations were therefore undertaken at the Hydraulics Laboratory of the National Research Council of Canada to study the propagation of Bounded Long Waves on a mild slope.

## 3.0 EXPERIMENTAL SET-UP

Investigations were carried out in a flume of dimensions 67 m x 1.2 m x 1.2 m (see Figure 1), equipped with a hydraulically driven wave generator operating in piston mode. The horizontal part of the flume in front of the wave paddle was 9 m long with a mean water depth of 0.7 m. A slope of 1:40 covering a distance of 17 m was used for shoaling purposes. This slope was then followed by a 16 m long horizontal part with a water depth of 0.28 m. A porous beach with a 1:30 slope was to dissipate wave energy at the end of the flume.

Considering wave length and velocity of these long waves, the experiments should ideally be carried out in very long flumes; however, such flumes are generally not available. Moreover, the distances used in this set-up represent some of the commonly encountered dimensions in model studies.

The shoaling slope and the following constant depth portion were constructed of sand covered with a thin layer of floated concrete. But subsequently the entire concrete surface had to be painted in order to make it smoother since preliminary investigations indicated a high degree of breaking and viscous loss due to the roughness of the bottom.

The permeable beach at the end of the flume was made up of 2 to 3 cm angular stones in order to allow the waves to penetrate through the stones and thereby dissipate as much energy as possible before being reflected at the vertical end of the flume. During a set of preliminary investigations a beach, with a slope of about 1:20 was originally used.

Under that set-up the results displayed a high degree of reflection, which could be detected particularly in the phases of long waves: in the first portion of the sampled record, the set-down and the corresponding set-up were properly reproduced but after about 50 s the phases were corrupted due to reflection.

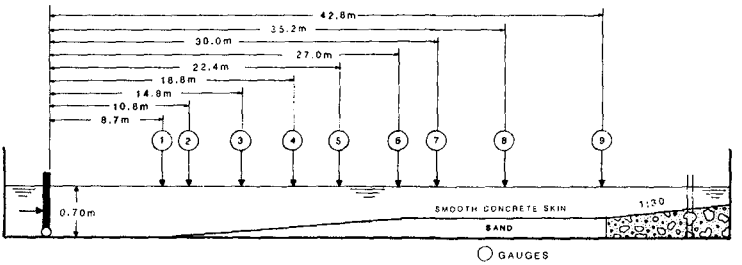


FIGURE 1

EXPERIMENTAL SETUP IN THE 4' FLUME

The slope used in this study (1:30) provided an optimum "effective length" of the flume and at the same time guaranteed satisfactory absorption characteristics. Given the limited lengths of the constant depth zones, a satisfactory reflection analysis could not be carried out in the present configuration.

A set of nine twin wire capacitance gauges were used to monitor the waves of the salient locations of the set-up. Wave generation and data acquisition were controlled by an on-line computer.

## 4.0 SELECTION OF TESTS

It has been shown by Barthel et al. (1) that the magnitude of bounded long waves and suppression terms used for the correct reproduction of bounded long waves change as a function of water depth and frequencies: higher amplitudes go with decreasing water depths and frequencies.

Since the amplitudes of the bounded long waves are generally very small in models ( a few mm), a careful selection of wave signals had to be done in order to obtain a distinct long wave with an amplitude well above the accuracy of the gauges and the signal noise level. As a result, a peak frequency of 0.43 Hz and a depth of water of 0.7 m were finally chosen since they provided reasonable amplitudes of the bounded long waves and at the same time an effective beach length for dissipation purposes. Jonswap spectra with three different characteristic wave heights (6 cm, 9 cm and 12 cm) were used on this study to establish the shoaling properties of the different amplitudes of the BLW. In addition, the amplitudes of BLW were varied by changing the grouping properties of the input wave which are described by the Groupiness Factor (GF), (Funke and Mansard) (3).

In a recent study Sand (7) has illustrated the direct relationship which exists between the bounded long wave and the Groupiness Factor. The Groupiness Factor, a measure of the wave group activity in a wave train, can be easily controlled in model tests using the synthesis techniques developed at the National Research Council of Canada (Funke and Mansard) (3). Using this technique, time series of 150 s with the same variance spectral density but with three different groupiness factors (GF = 0.60, 0.75 and 0.90), were synthesised. This resulted in three combinations of bounded long wave amplitudes for each characteristic wave height. Besides varying the groupiness factor, the synthesis technique, indicated above, could also be used to control the ultimate shape of the bounded long wave spectrum in terms of peak frequency and width. For this study, a relatively narrow spectrum with a peak frequency of 0.05 Hz was used. Complete details of the various steps involved in this technique are well documented in the reference cited above.

Data sampling was always initiated a few seconds before the generation in order to monitor corruption of bounded long wave, if any, due to reflections. However, in order to be consistent with the length of the time series used in generation, the analysis was carried out only for a period of 150 s. The generation technique was such that the same driving signal was recycled every 150 s which meant that any part of the time series with a length of 150 s could be used in the analysis. For this study, it was decided to sample for a total period of 325 s and analyse two portions of the record: one from 25 s to 175 s and another 175 s to 325 s. The choice of 25 s as initial time was based on the propagation time of the waves up to the 9th wave gauge. The results presented in this paper correspond generally to the first section of the record while the second portion was useful to establish the effects of reflections, if any.

One of the main objectives of this study, besides establishing the shoaling properties of BLW, is to investigate the effects of spurious long waves on the amplitudes of long wave oscillations measured in the shallow water region. Hence each combination of input sea states described above was run with and without compensation for spurious long waves.

The compensation for the spurious long waves was performed, as indicated in Section 1.0, by generating long wave components equal in amplitude but opposite in phases to the spurious contributions. Generation of the suppression terms often requires large paddle excursions as illustrated in Figure 2. The graph presents two driving signals used for the generation of the same input sea state ($f_p$ = 0.43 Hz, HCHR = 12 cm and GF = 0.9). The driving signal corresponding to the classical wave generation (without suppression) is shown in Figure 2a while Figure 2b displays the signal with correct compensations for spurious long waves.

## 5.0 ANALYSIS TECHNIQUES

The various analysis techniques used in this study, can best be described with the help of the illustrations presented in Figure 3 displaying a sample of analysis results obtained for the first gauge with and without compensation for spurious long waves.

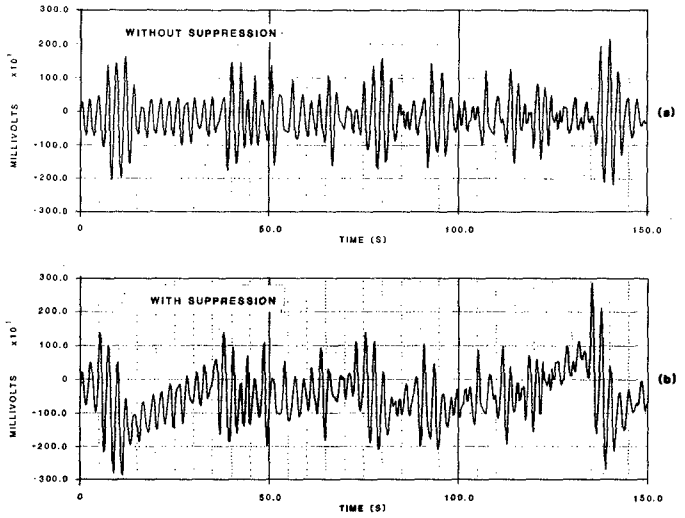


**FIGURE 2**

**DRIVING SIGNALS FOR AN IRREGULAR WAVE TRAIN WITH AND WITHOUT SUPPRESSION OF SPURIOUS LONG WAVES**

The wave train measured at the first gauge is shown together with the time series of measured and calculated long wave components. The spectra of these two long wave components are also presented in the same figure on the left hand side of the total spectrum.

The measured long waves (or the long waves prevailing in the model) were extracted from the total wave train by low pass filtering. Filtering was carried out using a time domain technique which convolved a data window with the input data. A 201 point Kaiser filter with a cut-off frequency 0.2 Hz was used for this purpose.

The expected (or calculated) long waves were obtained by theoretical relationships (Ottensen-Hansen et al.) (6) from the measured wave trains with a cut-off frequency excluding all the measured long waves (0.2 Hz).

Frequency domain analysis of these two long wave components and the measured wave train directly provided their corresponding spectral densities and RMS values. The closer the RMS value of the measured long waves is to the theoretical RMS value, the more successful is the spurious long wave suppression (see Fig. 3a). However, perhaps more important than matching the amplitudes of the measured long waves to their respective expected values, it is necessary to obtain a good agreement in phase. This is usually demonstrated by a distinct proper set-down and set-up of the mean water level with respect to the wave groups. Without any suppression, this agreement would be difficult to achieve

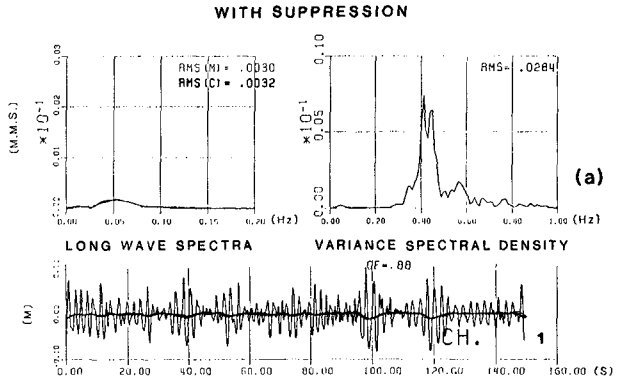


WAVE TRAIN WITH MEASURED AND CALCULATED

LONG WAVE COMPONENTS

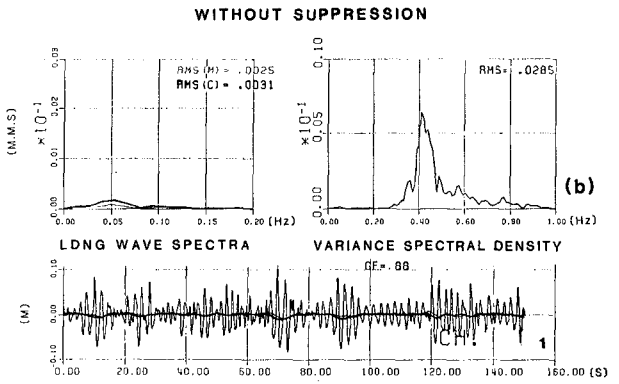


WAVE TRAIN WITH MEASURED AND CALCULATED

LONG WAVE COMPONENTS

FIGURE 3

ANALYSIS OF THE LONG WAVE CHARACTERISTICS

partly due to the differences in velocities between the free and bounded long waves. To verify the phase agreement between measured and calculated long waves, a cross correlation technique was used as follows:

$$C\eta_{LM}\eta_{LT}(\tau) = \frac{1}{T-\tau}\int_{-T/2+\tau}^{T/2} \eta_{LM}(t) \cdot \eta_{LT}(t+\tau)\,dt \Big/ \left(RMS\eta_{LT} \cdot RMS\eta_{LM}\right)$$

where, $\eta_{LT}$ = time series of theoretical (or calculated) long waves

$\eta_{LM}$ = time series of measured long waves

If optimum suppression is achieved, the analysis should indicate zero shift for maximum correlation. In practice the time shift $\tau$ (TAU) for maximum correlation is never quite zero. However, this variable proves to be a fair measure of success of suppression of spurious long waves. The maximum cross correlation coefficient is also never quite 1 due to small variations in the RMS values of the long waves which are very small themselves.

## 6.0 ANALYSIS OF RESULTS

### 6.1 Comparison Between Measured and Calculated Long Waves

Figure 4 presents comparisons between measured and calculated long waves for four different locations in the flume. To illustrate the effectiveness of suppression, results from both types of generation (with and without suppression) are also included in this figure.

The characteristics of the bounded long wave, measured at the first gauge before any shoaling took place, are illustrated in Figure 4a. The measured amplitudes and phases of the long waves show good agreement with theory when compensation was applied. On the other hand, when no compensation was done, the amplitudes and especially the phases of the BLW are different from the theoretical predictions. To a certain extent, this figure demonstrates not only the effectiveness of suppression but also the minimal influence of reflection: If reflections were higher, it would be difficult to obtain such a good match in spite of compensation.

The long waves measured, at gauges 3 and 5, during shoaling, are presented in Figures 4b and 4c. In the case of generation with suppression, the phase agreement between theoretical predictions and measured values are more or less maintained, but differences in amplitudes can be detected. When no suppression was included, differences between theory and experiment are much larger in amplitudes as well as in phases.

Since a large amount of breaking was taking place between probes 6 and 7, the long waves measured at gauge 9 (Fig. 4d) show very little correlation between theory and experiment. This is possibly due to the fact that the long waves measured at the 9th gauge are a superposition of two different contributions:

- long waves released by breaking process, and

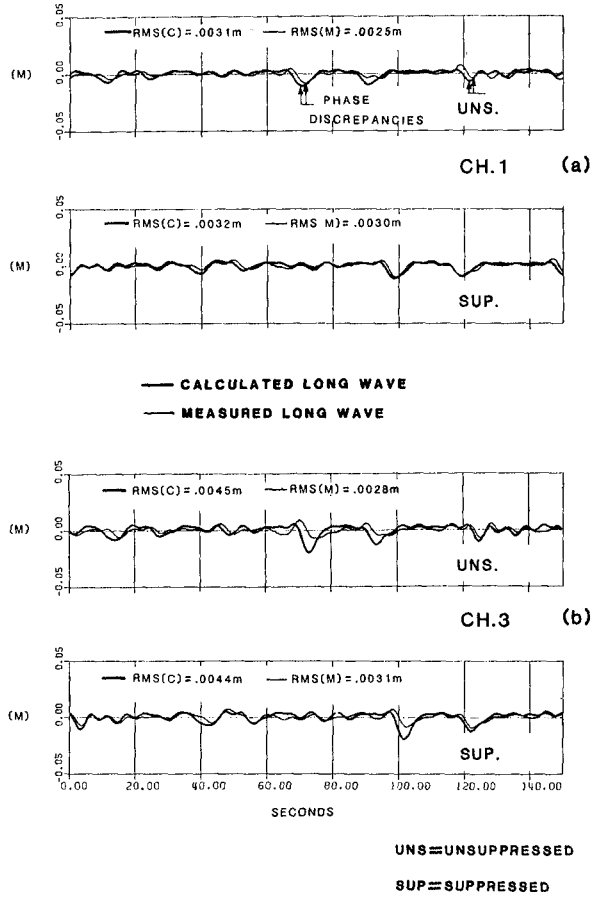


**FIGURE 4**

**COMPARISON OF MEASURED AND CALCULATED LONG WAVES**

SHORT WAVE SPECTRUM RMS=0.03m,GF=0.90

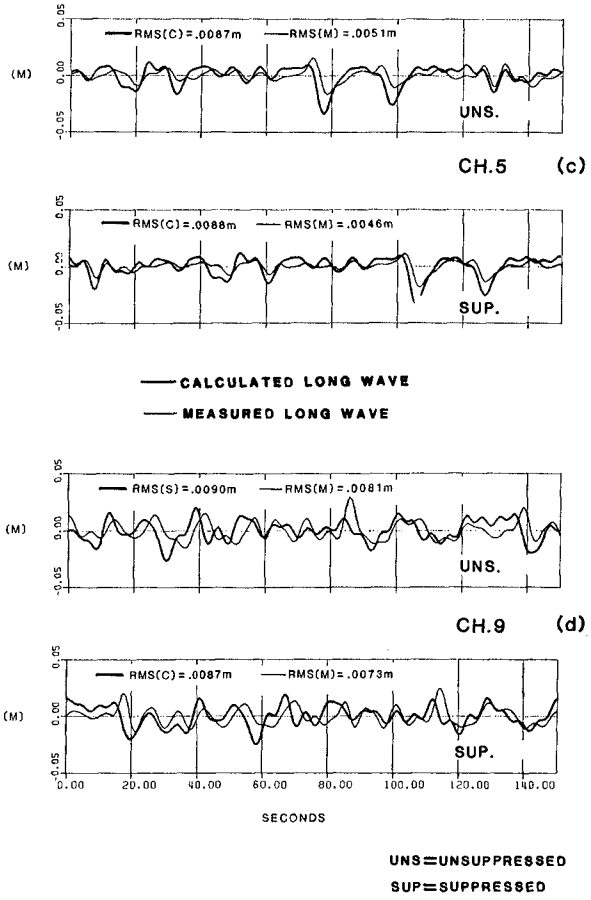


**FIGURE 4**

**COMPARISON OF MEASURED AND CALCULATED LONG WAVES**

SHORT WAVE SPECTRUM RMS=0.03m,GF=0.80

- long waves which are bound to a grouped wave train reconstituted after breaking.

The calculated long waves presented in these figures for various locations of the flume, were computed using the local depth of water. But it should be pointed out that the theoretical relationships available now are strictly valid only for a constant depth of water. Hence the predicitons which are presented here are only approximations of the true values. To calculate these true values it would be necessary to extend the existing theory by including terms for variable water depth and nonlinear interactions between first order and bounded long waves. Since, at present, such a theory is not available, the equations of Ottensen-Hansen et al. (6) provide a useful comparison to the various trends in BLW behaviour.

### 6.2 Amplitudes of the Measured Long Waves at Different Locations of the Flume

Figure 5 presents the variation of RMS values of the measured long waves along the flume. These results, only shown for the case of suppression of spurious long waves, illustrate very well some of the anticipated trends:

- The RMS value of the long waves increases with increasing wave height of the input sea state.

- For a given characteristic wave height of the spectrum (HCHR), an increase in GF results in large bounded long waves.

It is interesting to detect a reduction in the amplitudes of the long waves with increasing GF for the input sea states with HCHR = 9 and 12 cm at gauges 7, 8 and 9. This reduction could be attributed to the breaking of large waves due to the combination of high RMS value and large GF: a portion of the long wave energy could be expected to be dissipated with the breaking of short waves while the rest is released as free long waves.

Figure 6 presents a similar illustration of the amplitude of the long waves, but this time as a function of the amplitude of the measured short waves. With the amplitude of the long waves being proportional to the square of the amplitude of the primary wave train, the ratios of $RMS_{LW}/[RMS_{SW}]^2$ are illustrated in Figures 6a and 6b. Figure 6a represents the ratio of the expected long wave, while the values actually measured are displayed in 6b. Results of $RMS_{LWM}/[RMS_{SW}]^2$ suggest that, for both cases of generation (SUP and UNS), this ratio increases towards the end of the flume. While this increase could be associated with the shoaling effect in the sloped area, it is not clear as to why the same tendency prevails in the post-breaking zone where the depth is constant (gauges 7, 8 and 9). A possible explanation could be the superposition of the long wave energy released during breaking process with the group-bound energy of the post-breaking time series. It could also be partly due to incomplete stabilisation process after breaking.

Because of additional free wave energy, the generation process without suppression generally results in a higher value of this ratio within the shoaling process.

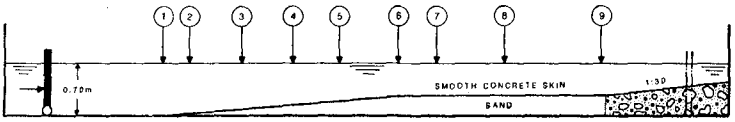


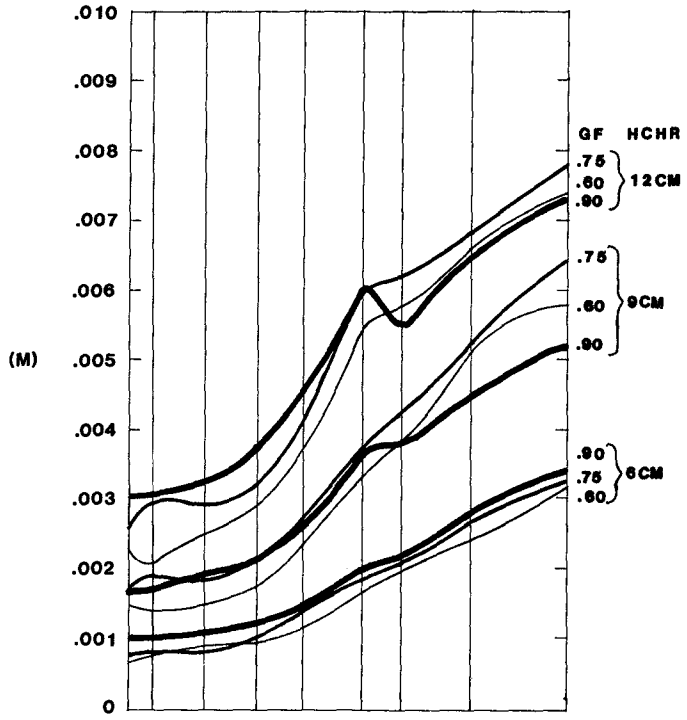


**FIGURE 5**

**RMS VALUES OF MEASURED LONG WAVES FOR 3 GF - VALUES AND 3 CHARACTERISTIC WAVE HEIGHTS OF THE SHORT WAVE SPECTRUM (SUPPRESSED)**

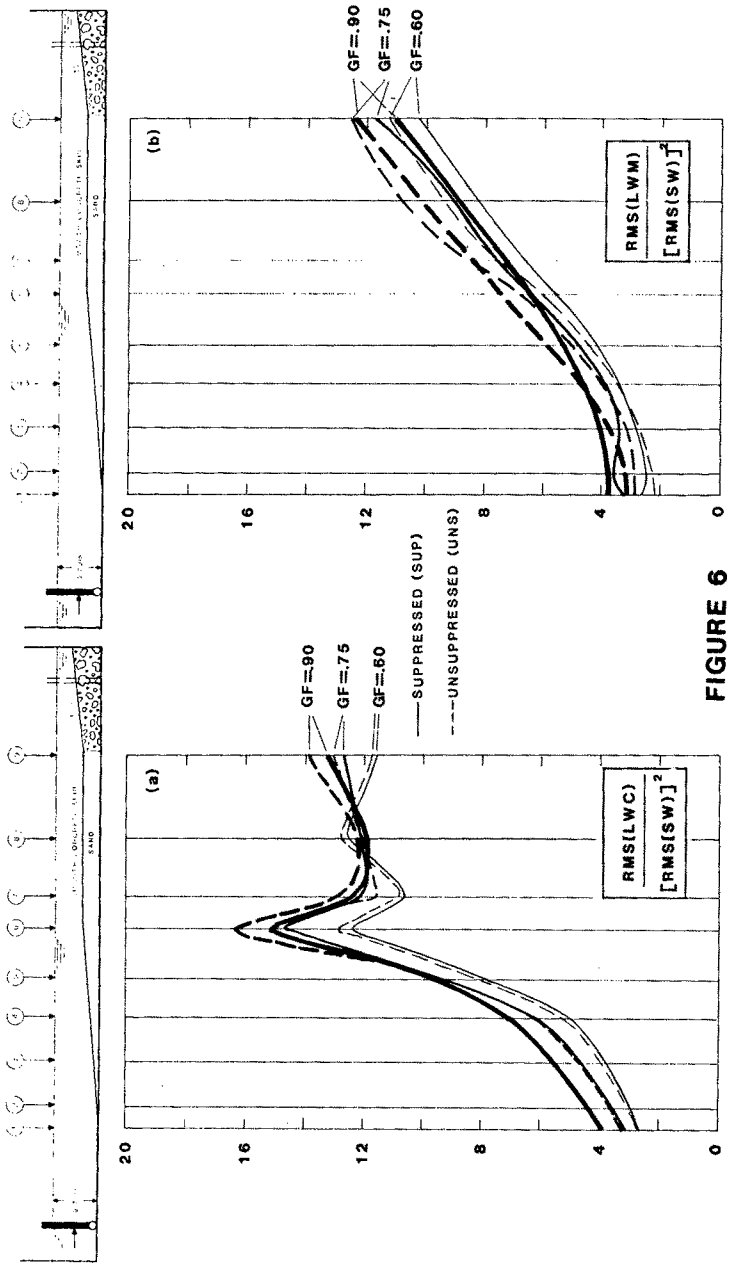


**FIGURE 6**

**RATIO $RMS_{LW}/[RMS_{SW}]^2$ (SUP.+UNS.)**

3 GROUPINESS FACTORS, RMS(SW)=0.03m

The ratio of expected long wave $RMS_{LWC}/[RMS_{SW}]^2$ increases much more rapidly on the slope than the measured one. In the post breaking zone, it decreases as anticipated to a more or less constant value. As discussed above, these variations are based on the estimations of the theoretical long wave. However, it is not clear why this ratio is slightly higher for the unsuppressed cases (2% on the average and 8% at probe 6). This appears to be partly due to slight changes in the spectral shape caused by the difference in breaking pattern. It has been observed that the omission of suppression causes waves to break in different regions than observed in the presence of correct suppression.

### 6.3 Cross-Correlation Between Measured and Theoretical Long Waves

The results of the cross-correlation analysis between measured and calculated long waves are presented in Figure 7. These results correspond to the input sea states of RMS = 0.03 m generated with different groupiness factors, each with and without suppression. The full lines indicate the suppressed case while the dotted lines represent the other. The effectiveness of suppression is well evident in this figure, since for all three groupiness factors the generation without suppression results in a poorer correlation and larger time shift as opposed to the generation with correct suppression. As anticipated, the correlation between theory and experiment decreases in the post breaking zone due to the superposition of energy from the bounded long waves and the long waves released by the breaking process. However, it is not clear why the time shift tends to decrease in that zone.

Similar cross correlation analyses were carried out to establish the effects of wave height of the primary spectrum and the influence of decreasing water depths.

As expected, a higher correlation and a smaller time shift value were achieved with lower wave heights resulting in less wave breaking.

With a shallower water depth (d = 0.6 m), the number of breaking waves was comparatively higher than in 0.7 m depth resulting in an increasing mismatch between expected and measured values. Distinctly higher phase shifts and lower correlation coefficients (TAU > 3 s and corr < 0.3 at gauge 7) reflected this result.

## 7.0 ENERGY BUILD-UP DUE TO REFLECTION

In order to establish the possible effect of reflection on the phases and amplitudes of BLW, the second portion of the record (175 s - 325 s) was subjected to similar analyses described above. The comparison of results of both portions of the records are presented in Figures 8 and 9 for two typical cases of GF. The cross-correlation between theoretical and obtained bounded long waves of both portions in Figure 8 show a good agreement in the TAU values while minor differences could be detected in the correlation coefficient. The match of the amplitudes of the long waves measured in different locations of the flume indicates a minimal effect of reflection (Fig. 9). In other words, the reflection coefficient was small enough not to substantially corrupt the progressive nature of the wave system in the set-up.

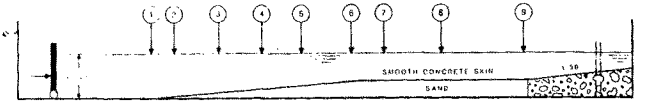


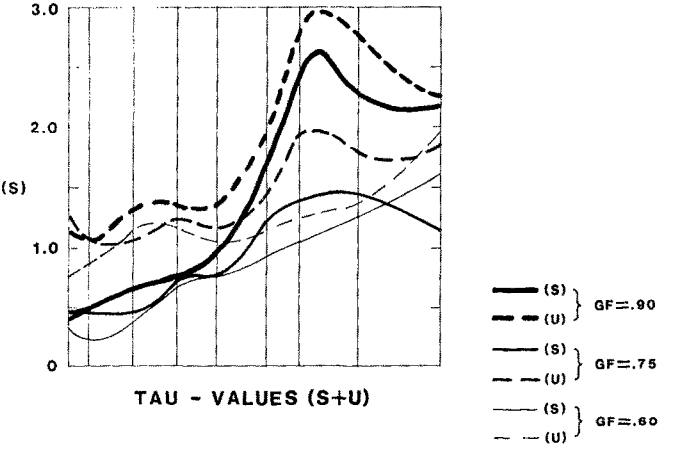


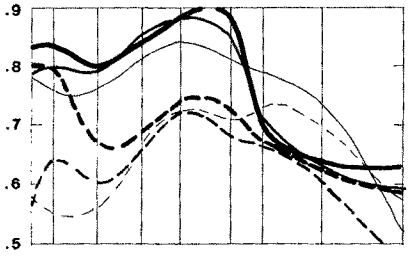


**FIGURE 7**

**TAU-VALUES AND CORRELATION COEFFICIENTS FOR DIFFERENT GROUPINESS FACTORS (SUP+UNS)**

SHORT WAVE SPECTRUM RMS=0.03m

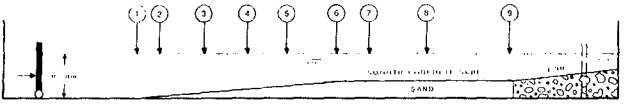


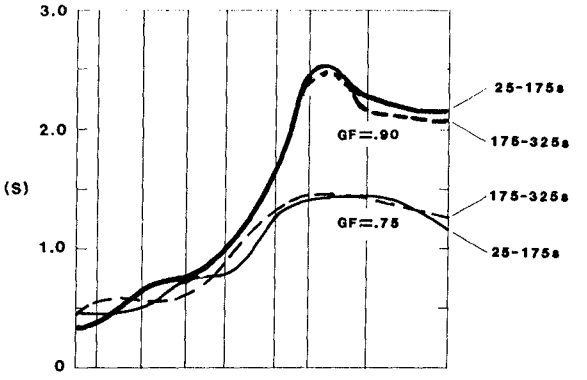


TAU-VALUE

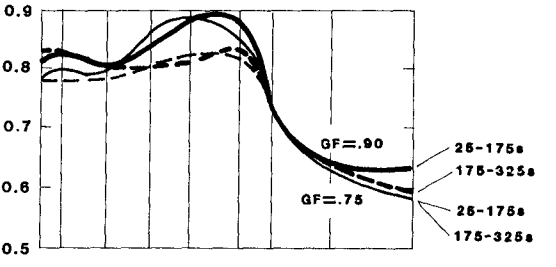


CORRELATION COEFFICIENT

FIGURE 8

TAU-VALUES AND CORRELATION COEFFICIENTS BEFORE AND AFTER REFLECTION BUILD-UP (SUP)

SHORT WAVE SPECTRUM RMS=0.03m

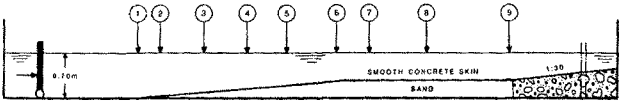


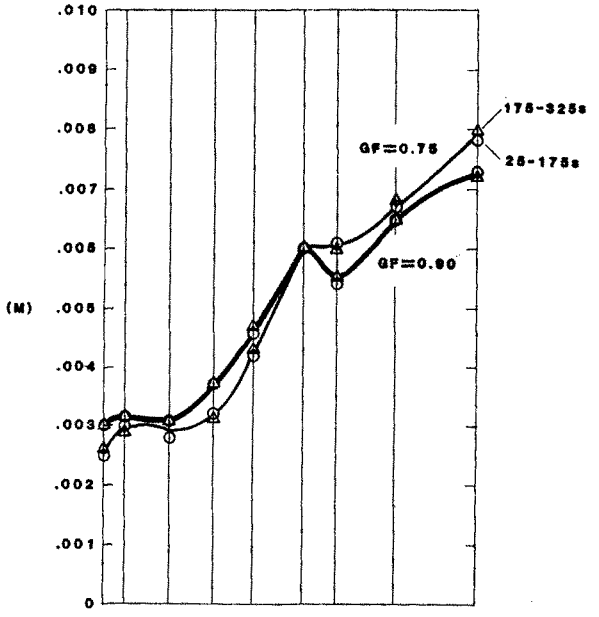


**RMS VALUES OF MEASURED LONG WAVES**

**FIGURE 9**

**LONG WAVE CHARACTERISTICS**

**BEFORE AND AFTER BUILD-UP (SUP)**

**SHORT WAVE SPECTRUM RMS=0.03m**

## 8.0 CONCLUSIONS

In the absence of a suitable theoretical description of bounded long wave propagation on a slope, this study provides useful experimental results on their shoaling properties. To date, the investigation suggests that

- there is a distinct trend in the increase of the BLW during shoaling.
- for nonbreaking waves, the relationship between BLW and GF is well documented.

In our experimental set-up, the classical wave generation, which does not include any suppression for spurious long waves, resulted in a higher magnitude of low frequency oscillations in the shallow region as opposed to those with suppression. However, this may not be true if the reflections had been high enough to set up a predominant standing wave pattern. Therefore it is recommended to suppress the spurious long waves in order to have a realistic model response. Further experiments are being carried out to study the effect of impervious beaches.

## 9.0 REFERENCES

1. Barthel, V., Mansard, E.P.D., Sand, S.E. and Vis, F.C., (1983), "Group Bounded Long Waves in Physical Models", Ocean Engineering, Vol. 10, No. 4.

2. Barthel, V., Mansard, E.P.D. and Funke, E.R., (1983), "Effect of Group-Induced Long waves on Wave Run-up", Proc. Coastal Structures 1983, ASCE, Arlington, U.S.A.

3. Funke, E.R. and Mansard, E.P.D., (1979), "On the Synthesis of Realistic Sea States", National Research Council of Canada, Hydraulics Laboratory Technical Report, LTR-HY-66.

4. Longuet-Higgins, M.S. and Stewart, R.W., (1964), "Radiation Stresses in Waver Waves, a Physical Discussion with Application", Deep Sea Research, Vol. 11.

5. Mansard, E.P.D. and Pratte, B.D., (1983), "Moored Ship Response in Irregular Waves", Proc. XVIII International Conference on Coastal Engineering, Cape Town, South Africa.

6. Ottensen-Hansen, N.E., Sand, S.E., Lundgren, H.., Sorensen, T. and Gravesen, H., (1980), "Correct Reproduction of Group-Induced Long Waves", Proc. XVII International Conference on Coastal Engineering, Sydney, Australia.

7. Sand, S.E., (1982), "Wave Grouping Described by Bounded Long Waves", Ocean Engineering, Vol. 9, No. 6.